EAN 2020
58th conference on experimental stress analysis

Pilot Study of Linear Localization Using the Acoustic Emission Method During a Semi-Circular Bending Test

TOPOLÁŘ L.[1, a]

[1]Brno University of Technology, Faculty of Civil Engineering, Veveří 331/95, 602 00 Brno, Czech Republic

[a]Libor.Topolar@vut.cz

Keywords: Linear localization, Acoustic emission method, Semi-circular bending test, Alkali-activated material, Crack formation

Abstract. The paper deals with the topic of linear localization of acoustic emission sources in fine-grained alkali-activated composites. The accuracy of the localization of acoustic emission events depends on the homogeneity of the environment with regard to the propagating ultrasonic waves. The pilot experiments were conducted on three placements of the acoustic emission sensors relative to the axis of the test specimen in a semi-circular bending configuration. The aim of these pilot experiments was to assess the influence of the acoustic emission sensor placement relative to the stress concentration on the localization of the acoustic emission events.

Introduction

The acoustic emission method is a very effective method for the detection of various levels of structural damage in different types of materials [1]. Accurate localization of acoustic emission sources can be used to derive crack initiation and propagation [2-4]. Substantial effort has been devoted to the study of accurate localization of acoustic emission sources and a number of algorithms have been devised to determine the source of acoustic emissions. These algorithms can be divided into two groups - non-iterative (they have the same velocity for all stations, so they are inflexible in dealing with variable velocity models) and iterative (the derivative method, the sequential search method, the genetic algorithm and the simplex method) [5-8].

The given algorithms are based on the assumption that acoustic waves propagate directly from the source to the sensor along a straight line. That is to say, the environment in which the waves propagate is sufficiently homogeneous for the generated acoustic waves. The described algorithms lose accuracy in the case of two distinct environments or in the case of refraction of the generated waves [9,10].

The pilot experiments involved linear localization of the acoustic emission sources. We focused on the influence of the sensor placement on the recorded localized acoustic emission events. At the same time, the experiments aimed to find the ideal placement for acoustic emission sensors relative to the stress concentration for a planned series of experiments.

Experiment description

The experiments were conducted in a semi-circular bending configuration [11]. The advantage of this configuration is the initiation of a tensile crack even under compressive load see Fig. 1 and photographs in Fig. 2. The experiment parameters were as follows:

- disk radius R = 50 mm,
- span between the supports S = 80 mm,
- notch length a = 25 mm,
- notch angle of inclination β = 50°.

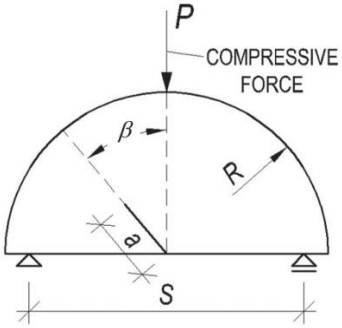

Fig. 1: Diagram of the semi-circular bending configuration used in the experiments [11]

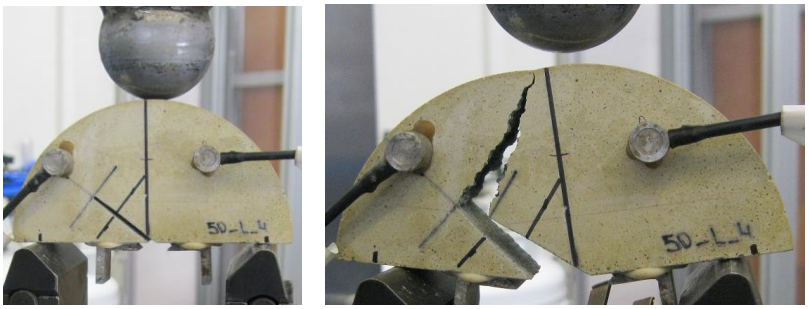

Fig 2: Photographs of the experiment before and after the fracture

The AE activity was observed by DAKEL-ZEDO system. DAKEL-ZEDO is a modular system for measuring AE that can be used throughout the entire spectrum of the application of this diagnostic method, for example, the detection and localization of the formation and development of the failure of materials. To measure this, the four-channel unit ZEDO-AE were used. The sensors were attached on the specimen surface with beeswax. The measuring AE parameters were set as follows frequency range 80–400 kHz; pre-amplifier 35 dB; software amplifier 20dB. The one sensor (guard-sensor) was mounted on the test equipment to catch the noise of background.

Results and discussion

The pilot tests were conducted on a fine-grained alkali-activated material. The dose of activator was adjusted to 6% Na_2O concerning the slag weight. Water to slag ratio was 0.45 (including water from the activator). Sand to slag ratio was 3:1 (by weight). Siliceous sand was with a grain size of up to 2 mm (consisting of three fractions according to EN 196-1). This fine-grained composite material is expected to contain minimal structural inhomogeneities that would prevent the passage of the generated mechanical waves. Three placements for the acoustic emission sensors were selected, see Figs. 3–5. Each sensor placement was subjected to determination of the localized position (vertical axis – the zero value is the position of the sensor that is in the notch section of the test specimen, left sensor) and amplitude of the acoustic emission (circle diameter) in relation to time. A graph of the course of the loading force in time is also presented.

In configuration A (Fig. 3), the sensors were placed symmetrically 30.0 mm from the axis of the test specimen. The left sensor, to which the distance of the localized events is related,

was at a direct distance of 17.7 mm from the end of the notch. The graph shows a cluster of localized events at the distance of 18.0 mm at the moment of reaching the maximum force. This cluster is probably connected to the formation of a crack emerging from the end of the notch. Later, more significant events are evident near the test specimen axis. This is related to the shift of the crack front towards the test specimen axis.

In configuration B (Fig. 4), the left sensor was placed 20.0 mm from the test specimen axis and the right sensor 30.0 mm from the test specimen axis. At the same time, the left sensor was at a direct distance of 14.0 mm from the end of the notch. In this configuration, it can be observed that no events near the end of the notch were localized at the moment of reaching the maximum force. This was probably caused by the small distance of one of the sensors from the end of the notch.

In configuration C (Fig. 5), the left sensor was placed 30.0 mm from the test specimen axis while the right sensor was placed 20.0 mm from the test specimen axis. The left sensor was therefore at the direct distance of 17.7 mm from the end of the notch, as in configuration A. An event was localised at the distance of 17.3 mm from the left sensor at the moment of reaching the maximum force and probably corresponds to the formation of a crack front. Other localized events again indicate the shift of the crack front towards the axis of the test specimen.

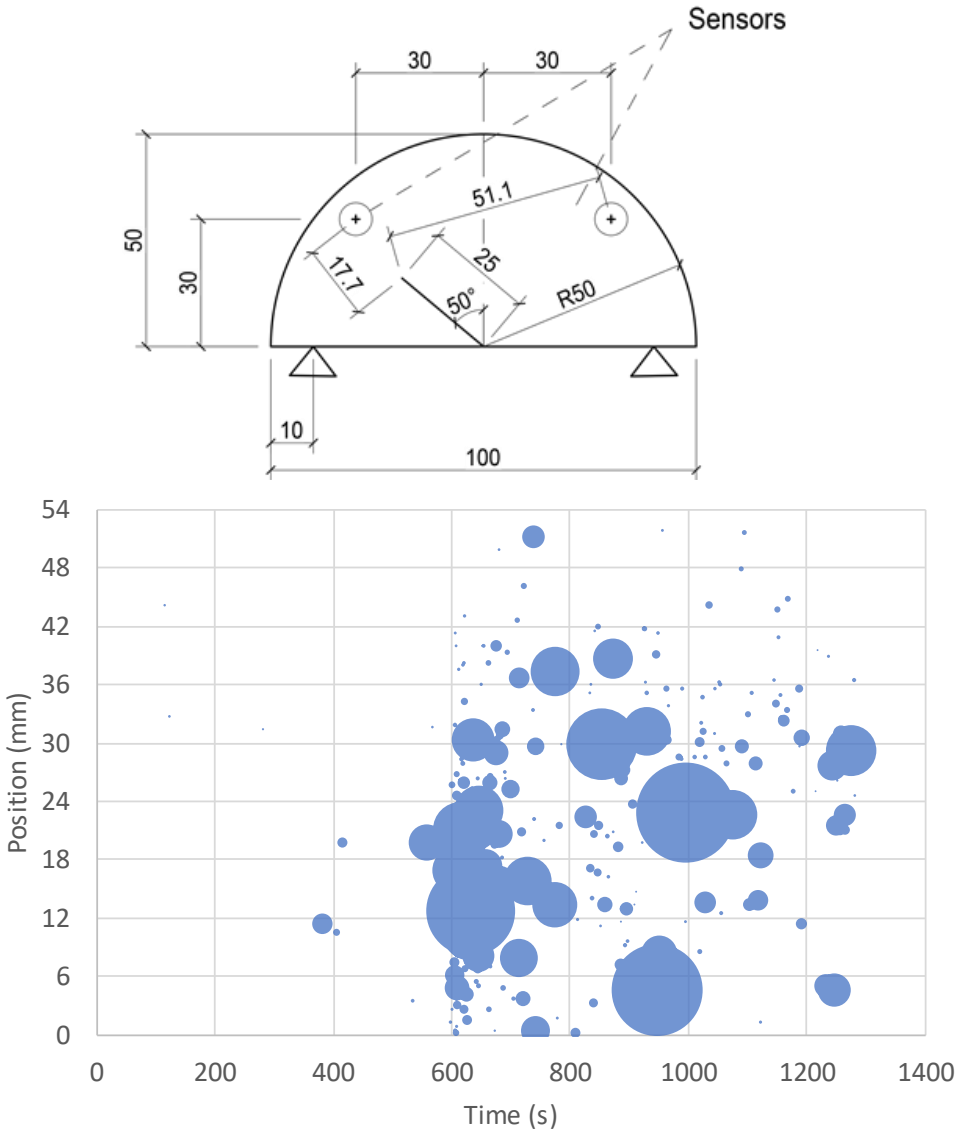

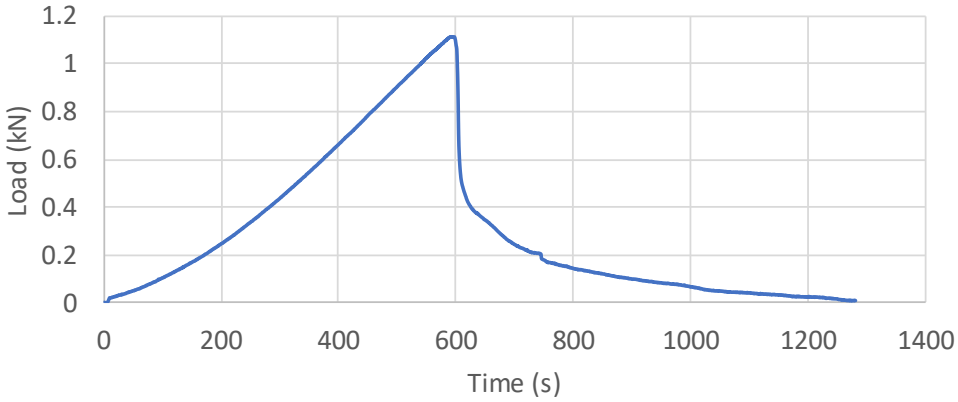

Fig. 3: Diagram of configuration A with results
(middle graph - vertical axis – the zero value is the position of the sensor that is in the notch section of the test specimen, left sensor)

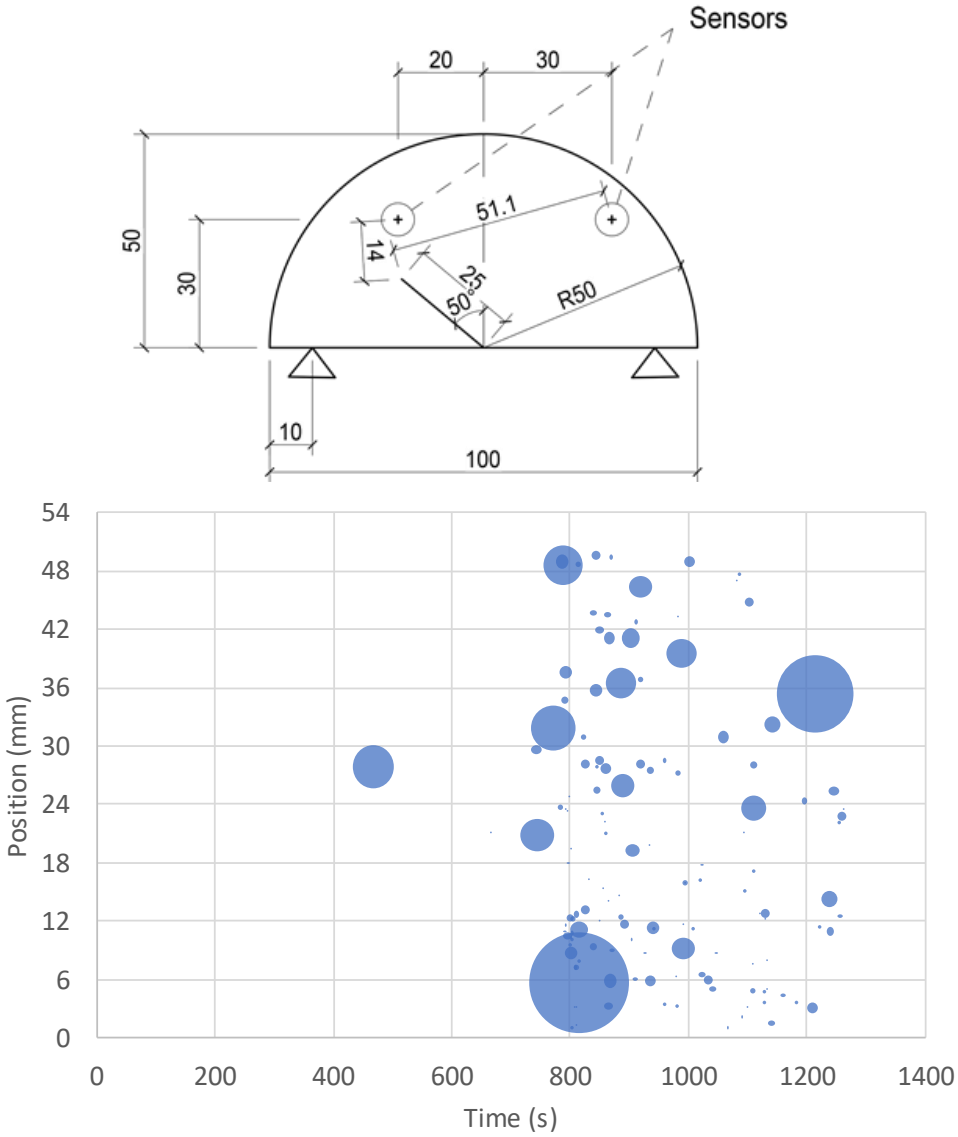

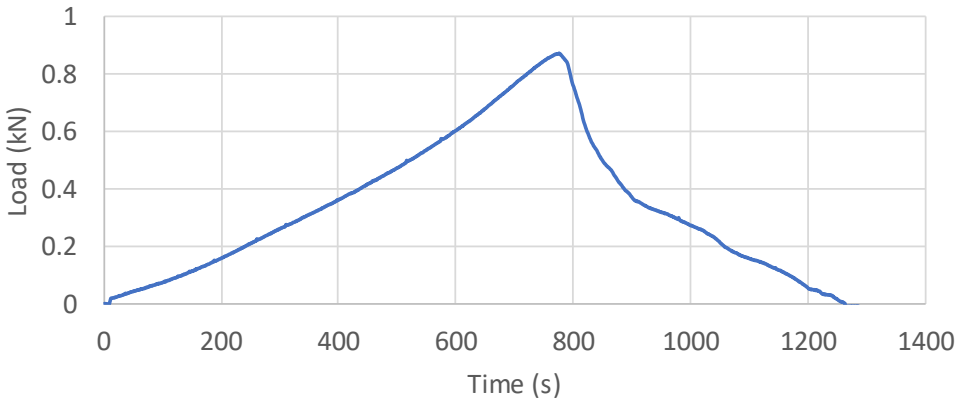

Fig. 4: Diagram of configuration B with results
(middle graph - vertical axis – the zero value is the position of the sensor that is in the notch section of the test specimen, left sensor)

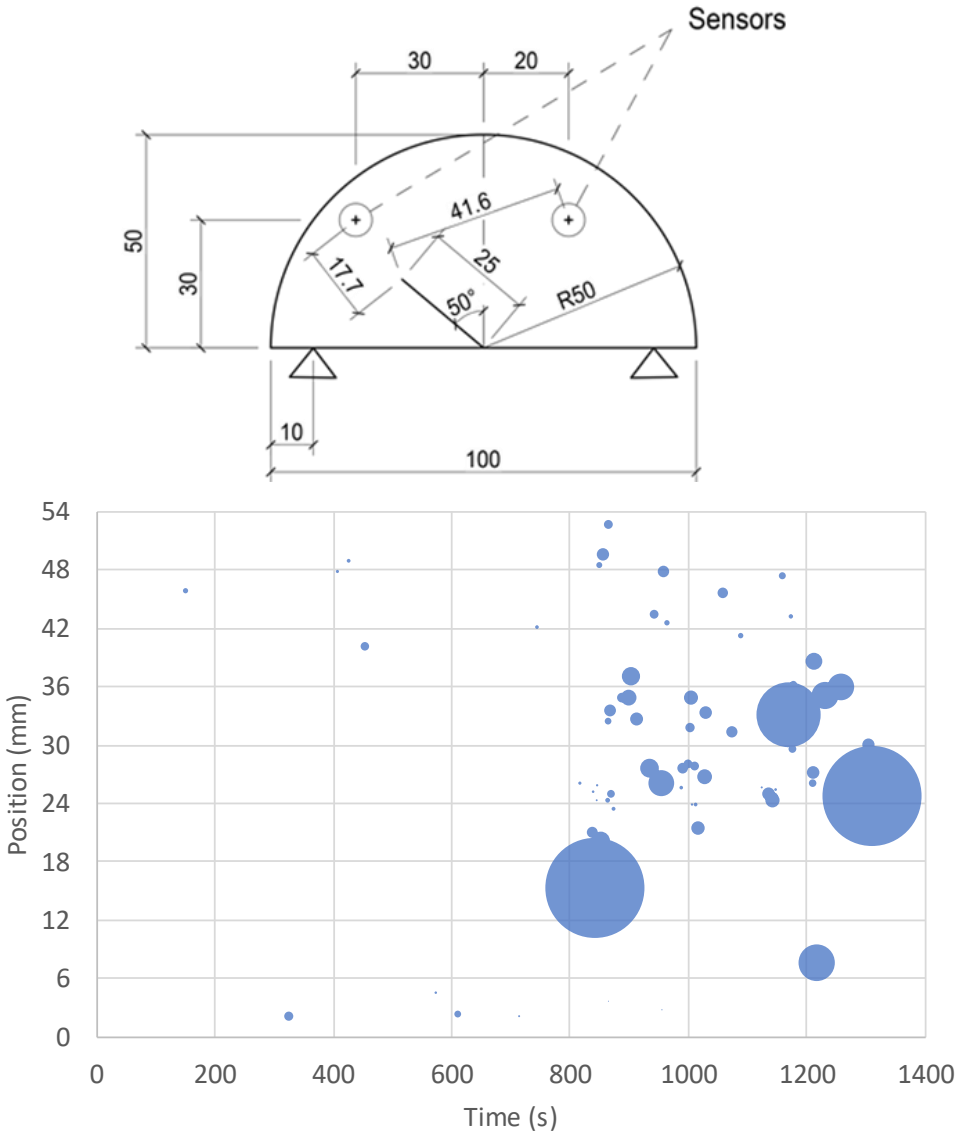

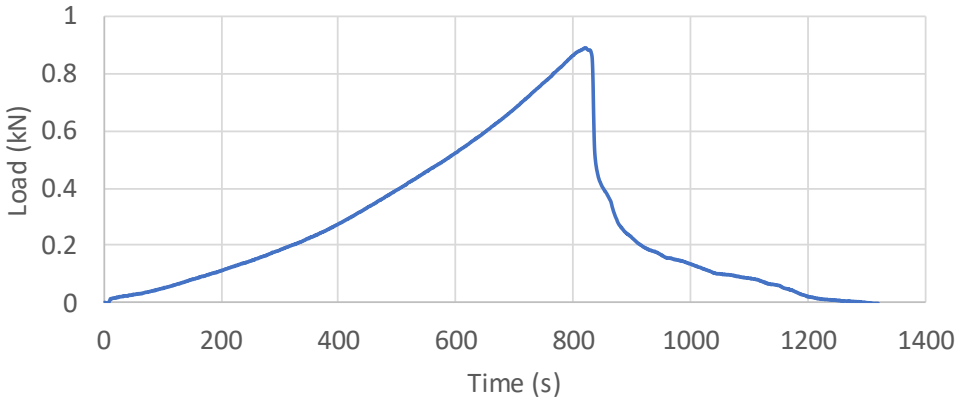

Fig. 5: Diagram of configuration C with results
(middle graph - vertical axis – the zero value is the position of the sensor that is in the notch section of the test specimen, left sensor)

Conclusion

The pilot experiments sought to identify a suitable position for the placement of the sensors in relation to the axis of the test specimen. Based on the results presented above, configuration B was discarded since it failed to successfully locate the acoustic emission events that would correspond to the theoretical assumption. The localized events also failed to match the physical outcome of the experiment. Configuration A was also discarded although its results were more consistent with both the theoretical assumption and the physical result. It was discarded because of a large number of false acoustic emission signals.

Configuration C was therefore selected for further experiments since the localized acoustic emission signals corresponded to both the theory and the physical result. At the same time, this configuration managed to filter out a large number of false signals. This is probably due to suitable distances of the individual sensors from the notch and from the axis of the test specimen.

Acknowledgement

This outcome has been achieved with the financial support of the Czech Science Foundation, project No. 18-12289Y “Advanced characterization of crack propagation in composites based on alkali activated matrix”.

References

[1] Ch.U. Grosse, M. Ohtsu (ed.), Acoustic emission testing, Springer Science & Business Media, 2008.

[2] M. Ohtsu, Prospective applications of AE measurements to infra-dock of concrete structures, Constr. Build. Mater. 158 (2018) 1134–1142.

[3] M.N. Noorsuhada, An overview on fatigue damage assessment of reinforced concrete structures with the aid of acoustic emission technique, Constr. Build. Mater. 112 (2016) 424–439.

[4] S.C. Paul, et al., Acoustic emission for characterising the crack propagation in strain-hardening cement-based composites (SHCC), Cem. Concr. Res. 69 (2015) 19–24.

[5] B. Debecker, A. Vervoort, Localization by acoustic emission in transversely isotropic slate, Adv. Acoust. Vib., 2011 (2011).

[6] W. Huang, W. Zhang, F. Li, Acoustic emission source location using a distributed feedback fiber laser rosette, Sensors 13.10 (2013) 14041–14054.

[7] Z. Zhou, et al., A new closed-form solution for acoustic emission source location in the presence of outliers, Appl. Sci. 8.6 (2018) 949.

[8] A.G. Beattie, Acoustic emission non-destructive testing of structures using source location techniques, Albuquerque and Livermore (2013).

[9] S. Sengupta, A.K. Datta, P. Topdar, Structural damage localization by acoustic emission technique: A state of the art review, Lat. Am. J. Solids. Stru. 12.8 (2015) 1565–1582.

[10] Z. Zhou, et al., Experimental study on the location of an acoustic emission source considering refraction in different media, Sci. Rep. 7.1 (2017) 1-13.

[11] L. Malikova, et al., Multi-parameter fracture mechanics, Frattura Integr. Strutt. 13.49 (2019) 65–73.